Displays 32 (2011) 296–307

Contents lists available at ScienceDirect

Displays

journal homepage: www.elsevier.com/locate/displa

Flexible-characteristics inspection system for flexible substrates by using image feedback control

Bor-Jiunn Wen [a,b], T.S. Liu [a,*]

[a] Department of Mechanical Engineering, National Chiao Tung University, Hsinchu 30010, Taiwan
[b] Center for Measurement Standards, Industrial Technology Research Institute, Hsinchu 30011, Taiwan

ARTICLE INFO

Article history:
Received 1 September 2010
Received in revised form 8 April 2011
Accepted 25 May 2011
Available online 12 June 2011

Keywords:
Flexible display
Flexible-characteristic inspection system
Polyethylene terephthalate/indium tin oxide substrate
Polyethylene terephthalate/hexamethyldisiloxane substrate
Image feedback control
Radius of curvature

ABSTRACT

The objective of this study is to present a new flexible-characteristic inspection system (FCIS) for measuring bending characteristics of flexible substrates under different bending conditions. In order to quantize bending conditions, charge-coupled device image feedback control is utilized to control radii of curvature of the flexible substrates. As a result, the new technique successfully measures electrical characteristics of flexible polyethylene terephthalate (PET)/indium tin oxide substrates up to 11,000 bending times by using FCIS. In addition, optical-transmittance characteristic measurement of PET/hexamethyldisiloxane substrates up to 5000 bending times under the same radius of curvature is implemented by using FCIS in this study. Inspection results of bending characteristics depicted on flexible displays help a designer or maker of flexible displays design useful and comfortable flexible electronic products.

1. Introduction

With rapid advance in semiconductor technology as well as in panel display industry, consumer product designs, including cellular phones, notebook computers, monitor display, and other digital household appliances are becoming more and more diversified. However, stiff panel displays cannot satisfy people who demand comfortable lifestyle. Flexible displays, which are thin, flexible, light, and shock-resistant, become the top choice in consumer products. The fabrication of displays on the flexible substrates requires the deposition of functional coatings which serve as electrical conductors, barriers to moisture permeation, mechanical protection, or backplane electronics, i.e., thin-film transistors (TFT). Display devices are expected to be large-area rollable sheets. Although several deformation geometries of conforming substrates are possible, i.e., hemispherical cap, helix, twisting, etc., the simplest configuration that a rollable device must be able to withstand is bending around a cylinder of a given radius. Therefore, testing of flexible displays under different deformation geometries will play an important role in research and production.

Dealing with flexible displays, Grego et al. [1] evaluated two measurement systems, each with different advantages in bending test capability: a collapsing radius system [2] and an X–Y–θ bending system [3]. In the collapsing radius set-up, the bending shape is, however, not exactly cylindrical and a numerical study [4] concluded that, assuming perfectly elastic behavior, the minimum bending radius experienced by the sample is 20% smaller than the half plate-distance. In the X–Y–θ system, it takes more time for positioning X, Y, and θ coordinates of every bending radius. If there is an error for control, it might damage the sample. In addition, both three-point bending and four-point bending are experiments commonly used in the industry. Chen et al. [5] provided a new modified method of three points bending in the test. In a similar manner, the collapsing radius system has around 20% error in bending radius.

So far, existing equipments and standards can only test for larger radii or folding conditions of the sample and cannot inspect bending characteristics of optical, mechanical, and electrical characteristics under bending situations. It is therefore desirable to develop a testing system, a measurement, and analysis methods that enable testing over a wide range of bending radii and are capable of quantizing more accuracy of bending situations for measuring the bending characteristics of a thin-film-coated substrate. The purpose of this study is to put forward a new flexible-characteristic

* Corresponding author. Address: 1001 Ta-Hsueh Road, Hsinchu 30010, Taiwan. Tel.: +886 3 5712121x55123; fax: +886 3 5720634.
E-mail address: tsliu@mail.nctu.edu.tw (T.S. Liu).

0141-9382/$ - see front matter © 2011 Elsevier B.V. All rights reserved.
doi:10.1016/j.displa.2011.05.008

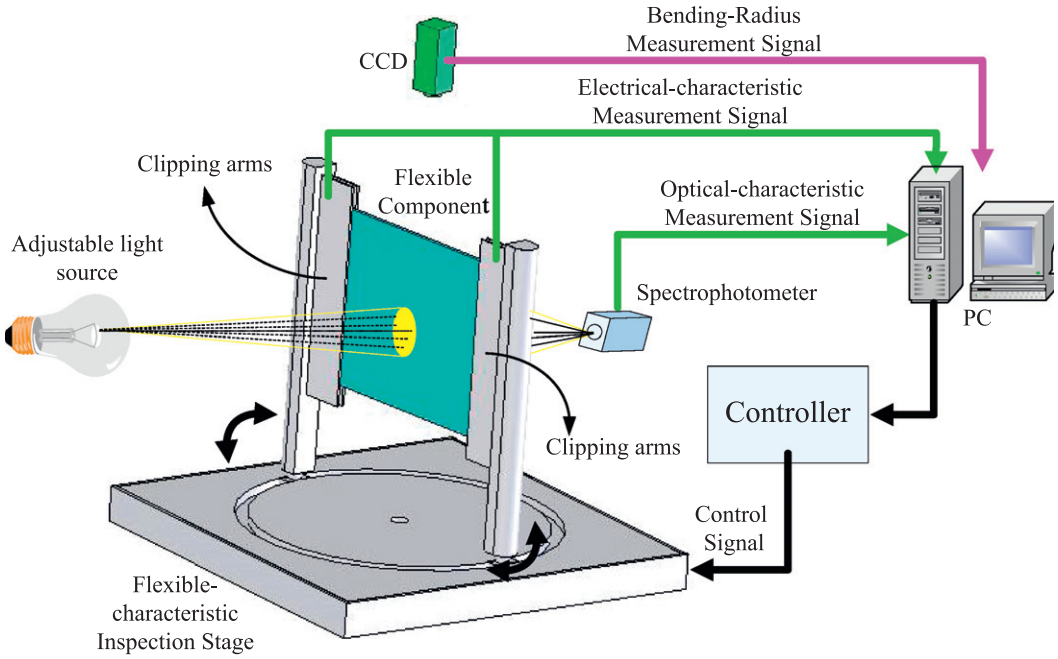

Fig. 1. Flexible-characteristic inspection system.

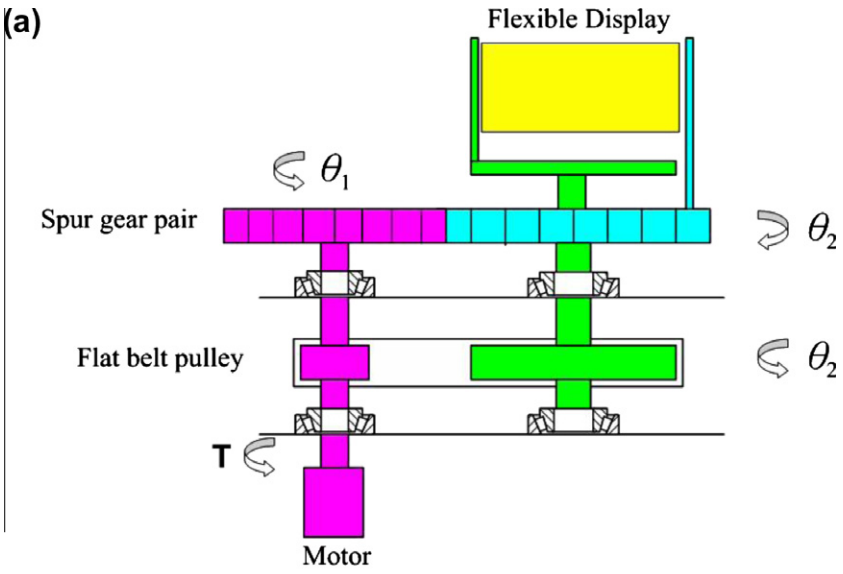

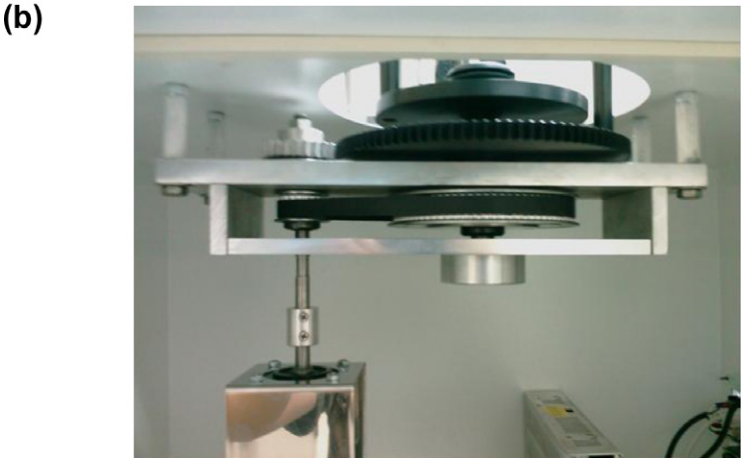

Fig. 2. (a) Design diagram of actuation mechanism and (b) photo of actuation mechanism.

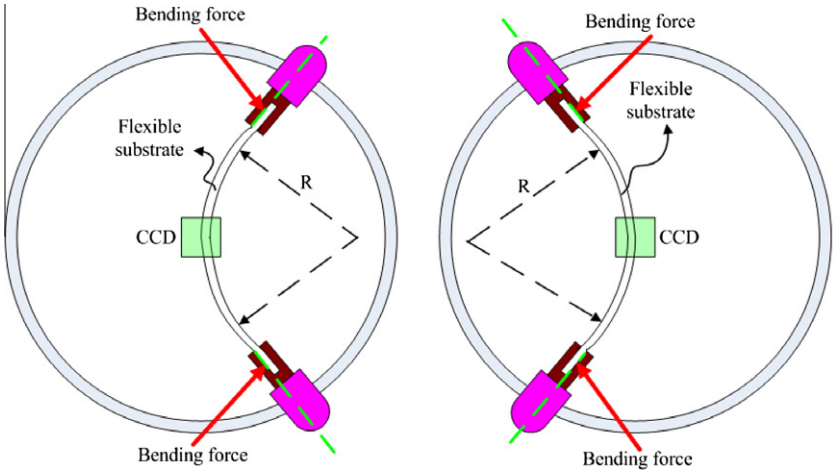

Fig. 3. Bending force measurement apparatus of FCIS in top view.

inspection system (FCIS) for measuring bending characteristics of the flexible substrate under different radii of curvature. This FCIS is designed to exert an external bending force on the flexible substrate. It results in a curved substrate, which is taken by a charge-coupled device (CCD). FCIS is used to carry out image processing using a LabVIEW software, calculate the radius of curvature of the flexible substrate, utilize the CCD image feedback control (IFC) to control the radius of curvature of the flexible substrate, and measure bending characteristics. This study deals with polyethylene terephthalate (PET)/indium tin oxide (ITO) substrate up to 11,000 bending times by using FCIS, and measures electrical characteristics.

In addition, hexamethyldisiloxane (HMDSO) plasma-polymerized thin films can be used for a large number of applications in rather different fields such as low-k dielectric layers for microelectronic applications, barrier films for food and pharmaceutical packaging, corrosion protection layers, coatings for biocompatible materials, and protective anti-scratch coatings on plastic substrates for flexible displays [6–8]. Therefore, optical-transmittance characteristic measurement of flexible PET/HMDSO substrates up to 5000 bending times under the same radius of curvature is implemented by using FCIS in this study. These inspection results of bending characteristics depicted on flexible displays help a designer or maker design useful and comfortable flexible display product.

2. Flexible-characteristic inspection system

2.1. Structure of FCIS

To measure bending characteristics of the flexible substrate requires a stable inspection system. In existing reference papers, equipments and standards, although the collapsing radius system is often used to test the flexible substrates, it is difficult to control the bending radius. The initial (mounting) radius must be sufficiently larger than the one corresponding to the onset of cracking of the substrate coating. The collapsing radius system also cannot measure the planar characteristics of the flexible substrates. Therefore, this study puts forward an FCIS to generate bending in the flexible-substrate test, as shown in Fig. 1. FCIS can measure the planar and bending characteristics of the substrates. The initial (mounting) condition of the substrate is planar and not to damage it. FCIS for inspecting characteristics of the substrates, comprises a clipping device, a flexible-characteristic inspection stage with a moving controller, a computer, and a CCD camera. In addition, the clipping device is configured with two clipping arms which can work cooperatively to hold a substrate. In order to bend the substrate, this study designed an opposite moving of two clipping arms in the round moving simultaneously to implement. Fig. 2a is the design diagram of the actuation mechanism for an opposite moving of two clipping arms in the round moving simultaneously. The servo motor drives the flat belt pulley and the spur gear pair in the same speed simultaneously. The flat belt pulley and the spur gear pair link up different clipping arms, respectively. According to the design of the actuation mechanism, the transmission speed from the servo motor to the flat belt

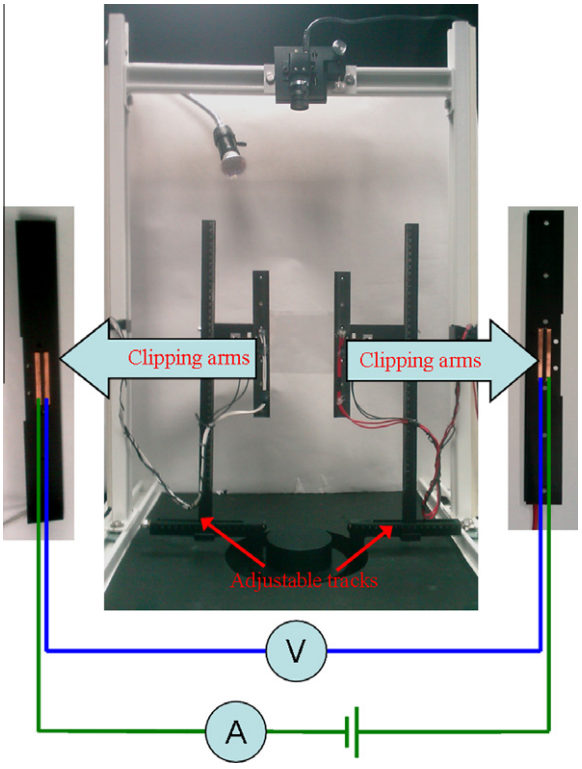

Fig. 4. Four-point-probe electrical-resistance measurement apparatus.

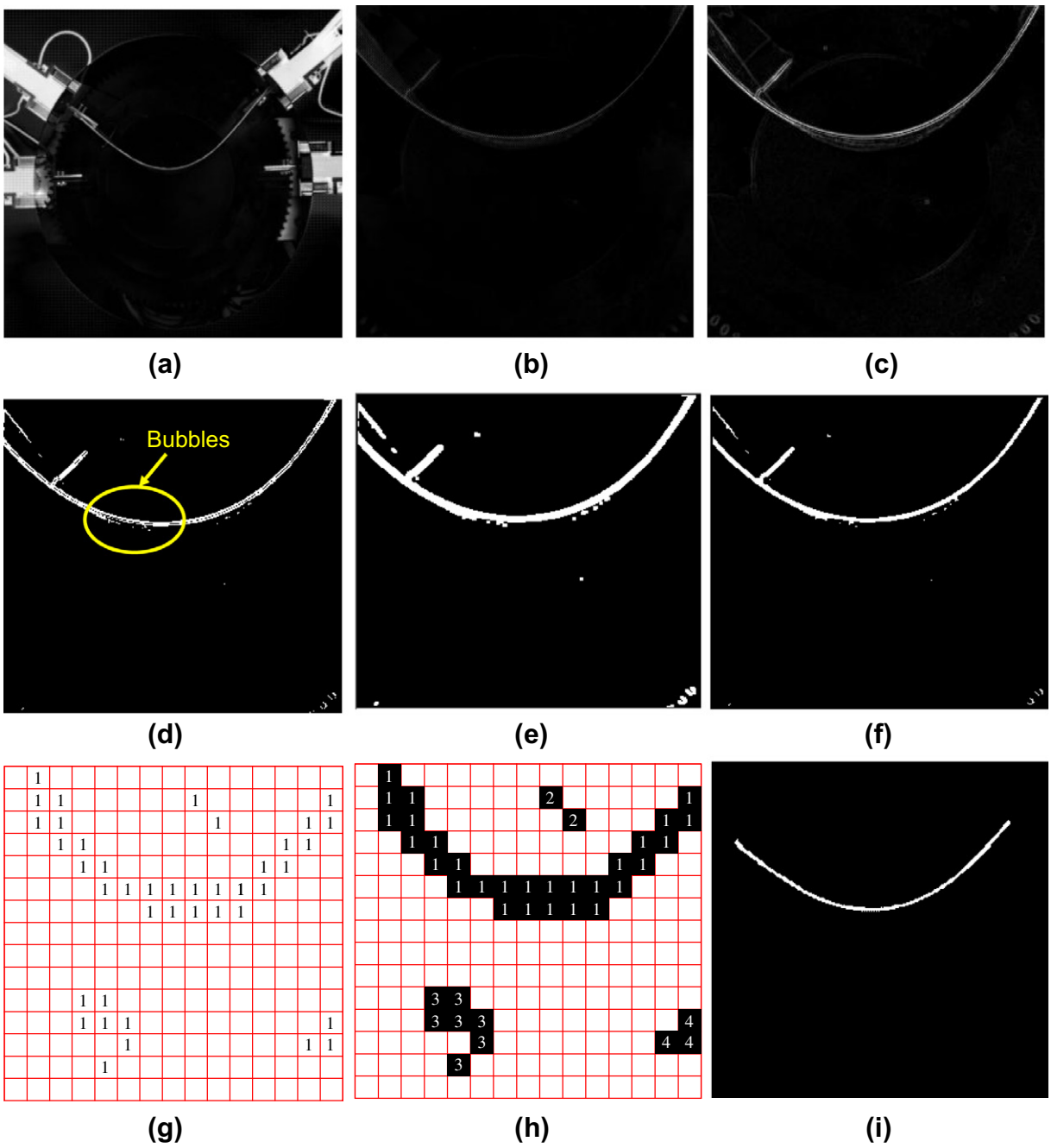

Fig. 5. Profile image of the substrate: (a) after using background subtraction, (b) mask filter, (c) Sobel mask, (d) after image thresholding, (e) after dilation operation, (f) after erosion operation of image of the substrate profile by using the closing operation, (g) first pass, (h) second pass processes of connected substrate labeling for the image of the substrate profile, and (i) image of the substrate profile after six-step image processing.

pulley is the same as to the spur gear pair, but in opposite directions respectively. Therefore, both clipping arms can make an opposite movement of the two clipping arms in the circular path at the same moving speed simultaneously by the actuation mechanism of FCIS, as shown in Fig. 2b. Moreover, because there is only a bending force on the perpendicular direction of the substrate by clipping arms, as shown in Fig. 3, an opposite movement of the two clipping arms in the circular path simultaneously can bend the substrate.

In addition, to measure electrical characteristics of the substrate in bending requires an electrical-resistance measurement apparatus. Hence, this study designs a clipping device with a 4-point-probe electrical-resistance measurement apparatus. The clipping device comprises two clipping arms and two adjustable tracks. In order to measure electrical-resistance characteristics, the 4-point-probe resistance measurement apparatus is integrated into two clipping arms, as shown in Fig. 4. There are two electrodes on each clipping arm. Errors of the electrode-contact electrical-resistance are reduced by using the principle of the 4-point-probe electrical-resistance measurement [9]. Moreover, both tracks are used to adjust the clipping arms in order to firmly hold a sample.

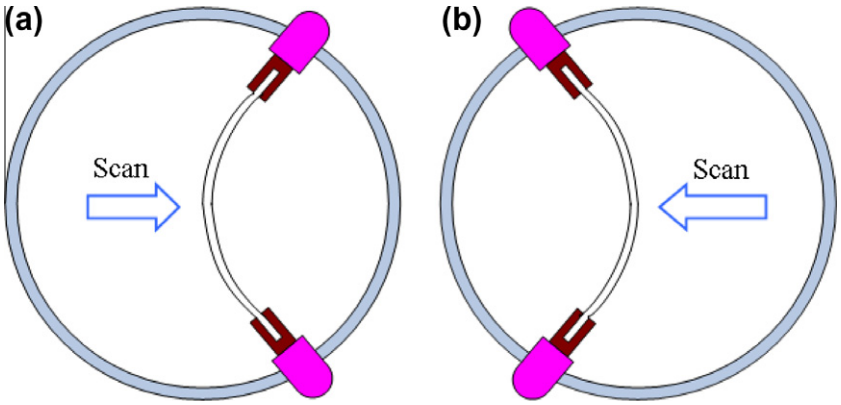

Fig. 6. (a) Left-convex profile and (b) right-convex profile scanning methods used to transform substrate image into coordinates.

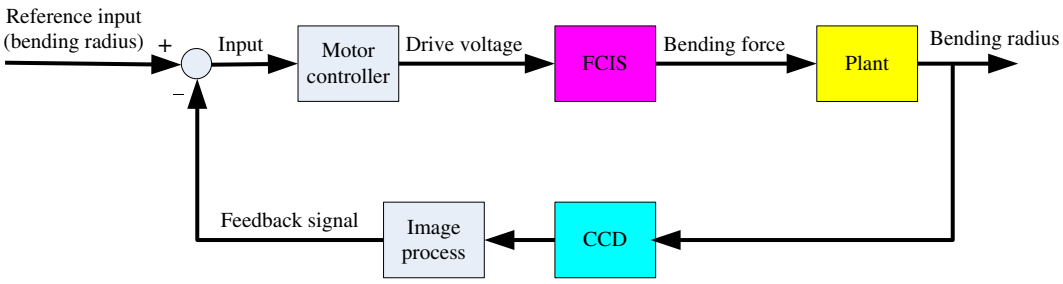

Fig. 7. Control block diagram.

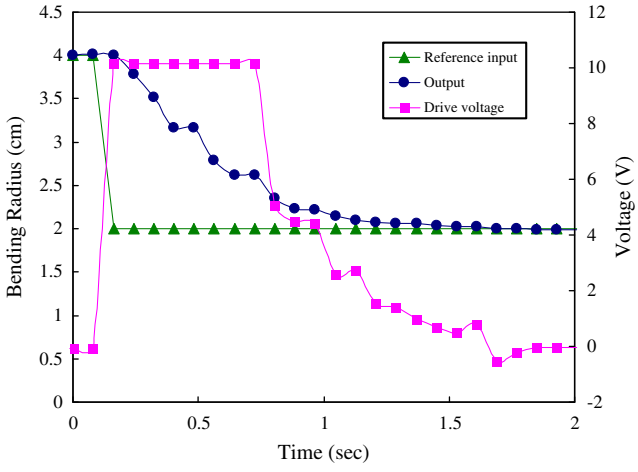

Fig. 8. Bending radius and input voltage in experimental results of bending radius variation from 4 to 2 cm.

2.2. Measurement for radius of curvature of flexible substrate

In order to quantize the bending condition, a CCD camera is used to shoot the top-view edge image of the substrate, and carry out image processing to measure the radius of curvature of the substrate in seven-step image processing.

2.2.1. Image sampling and quantization

Top-view edge images of the substrate belong to RGB images, which have to be transformed into grayscale images first before image processing. Dealing with the top-view contour image of the substrate, one has to convert its continuous sensed data into digital form. Assume that an image $f(x, y)$ is sampled, so that the resultant digital image becomes an M rows and N columns matrix.

2.2.2. Background subtraction

Calculate the bending radius requires a clear top-view edge profile image of the substrate. Hence, background subtraction [10–12] is used to extract the noiseless profile image of the substrate from the top-view edge image. Firstly, this study sets up a sampling and quantization of digital background image by CCD. Secondly, this study uses the background subtraction to subtract background image from the real-time top-view edge image. The resultant image is shown in Fig. 5a. Then, a mask is utilized to filter the profile image of the substrate from the subtraction image, as shown in Fig. 5b.

2.2.3. Edge detection

Because substrates are generally made from transparent materials, edge detection of the profile image is an unusual task. After extracting the profile image of the substrate, there is still some noise and weakness edge image on it. In order to enhance the edge image with less noise, gradient operators [13–15] were utilized. Hence, a Sobel mask [16] is utilized for enhancing the edge detection in this study. Fig. 5c depicts the substrate image after using the Sobel mask.

2.2.4. Otsu's law thresholding

After the edge detection is enhanced, the profile image of the substrate is gray-level image, which needs a lot of memory for storing in a computer and is difficult to extract the profile of the

Table 1
Results of 1 and 2 cm bending radius control for 75 × 75 mm and 125 × 125 mm PET substrates, respectively, by using IFC.

Bending times	Bending conditions	
	1 cm bending radius for 75 × 75 mm substrate (cm)	2 cm bending radius for 125 × 125 mm substrate (cm)
0	0.99	1.98
500	1.00	1.97
1000	0.96	1.97
2000	0.95	1.97
3000	0.95	1.97
4000	0.95	1.97
5000	1.01	1.98
6000	0.99	1.97
7000	1.05	1.98
8000	1.05	1.97
9000	1.01	1.98
10,000	0.99	1.97
11,000	0.95	1.97

substrate. Hence, image thresholding is applied. This study uses Otsu's law [17] to estimate threshold. After Otsu's law thresholding is carried out, Fig. 5d depicts the image thresholding of the substrate profile.

2.2.5. Morphological operations

As depicted in Fig. 5d, there exist some bubbles in the substrate profile. It is thus difficult to calculate the bending radius by using the substrate profile with the bubbles. In order to solve the problem, morphological operations [18] are utilized in this study. After using the closing operation for Fig. 5d, the substrate profile obtains a clearer image, as shown in Fig. 5e and f.

2.2.6. Connected component labeling

After using the closing operation, there is still some noise in the image of the substrate profile. In order to reduce the noise, connected component labeling is employed. A two-pass algorithm [19] iterates through two-dimensional, binary data. The algorithm makes two passes over the image: one pass to record equivalences and assign temporary labels and the second to replace each temporary label by the label of its equivalence class.

On the first pass:

1. Iterate through each element of the data by column, then by row.
2. If the element is not the background.
   a. Get the neighboring elements of the current element.
   b. If there are no neighbors, uniquely label the current element and continue.
   c. Otherwise, find the neighbor with the smallest label and assign it to the current element.
3. Store the equivalence between neighboring labels.

On the second pass:

1. Iterate through each element of the data by column, then by row.
2. If the element does not belong to the background.
   a. Relabel the element with the lowest equivalent label.

The process of the connected component labeling for the image of the substrate profile is shown in Fig. 5g and h.

According to Fig. 5g and h, all of the noise patterns are smaller than the substrate profile. To remove the noise, a size filter is used to filter the label of small area. Finally, the noiseless image of the substrate profile is obtained, as shown in Fig. 5i.

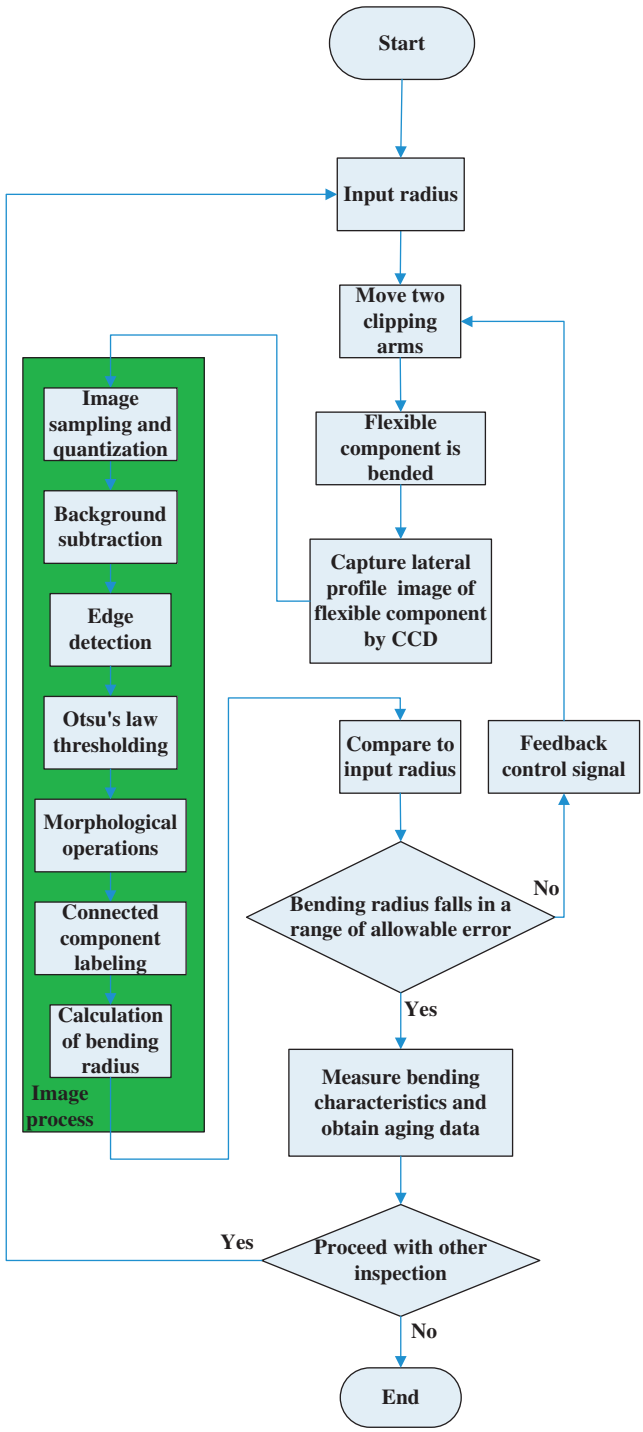

Fig. 9. Flowchart of measuring electrical characteristics of flexible PET/ITO sample.

2.2.7. Calculation of bending radius

In order to quantize the bending condition, calculating the bending radius is a key technique. To calculate the bending radius requires noiseless images of the substrate profile. After image processing for obtaining the noiseless images of substrate profiles, a scanning method is executed to obtain coordinates of the substrate

Table 2
Aging results in electrical-resistance measurement of 30 dpi flexible PET/ITO sample in flat and 2 cm bending radius conditions up to 11,000 bending times.

Bending times	Bending conditions			
	Flat		2 cm bending radius	
	Bending radius (cm)	Resistance (kΩ)	Bending radius (cm)	Resistance (kΩ)
0	∞	9.579	1.98	9.584
500	∞	9.597	1.97	9.601
1000	∞	9.607	1.97	9.613
2000	∞	9.620	1.97	9.623
3000	∞	9.623	1.97	9.631
4000	∞	9.629	1.97	9.633
5000	∞	9.627	1.98	9.636
6000	∞	9.630	1.97	9.636
7000	∞	9.635	1.98	9.639
8000	∞	9.637	1.97	9.643
9000	∞	9.640	1.98	9.643
10,000	∞	9.645	1.97	9.651
11,000	∞	9.649	1.97	9.654

profile, as shown in Fig. 6. When the substrate is bent for a left convex, the image of the substrate profile is transformed into coordinates from left to right by image processing, whereas it is transformed into coordinates from right to left for a right-convex bend. With all the coordinates of the substrate profile, curve fitting is carried out by using

$$x^2 + y^2 + Cx + Dy + E = 0 \tag{1}$$

where C, D and E are the parameters of the curve fitting equation. M set coordinates of the substrate profile are obtained by the scanning method. Substituting coordinates (x_m, y_m) into Eq. (1) yields

$$\begin{bmatrix} x_1 & y_1 & 1 \\ x_2 & y_2 & 1 \\ \vdots & \vdots & \vdots \\ x_m & y_m & 1 \end{bmatrix}_{m\times 3} \begin{bmatrix} C \\ D \\ E \end{bmatrix}_{3\times 1} = \begin{bmatrix} -x_1^2 - y_1^2 \\ -x_2^2 - y_2^2 \\ \vdots \\ -x_m^2 - y_m^2 \end{bmatrix}_{m\times 1} \tag{2}$$

Eq. (2) is written as

$$A_{m\times 3} X_{3\times 1} = B_{m\times 1} \tag{3}$$

A least square algorithm

$$X = (A^* A)^{-1} A^* B^* \tag{4}$$

is used to solve Eq. (3). Substituting the solution of Eq. (4) into Eq. (1) gives

$$\left(x - \frac{C}{2}\right)^2 + \left(y - \frac{D}{2}\right)^2 = \frac{C^2}{4} + \frac{D^2}{4} - E = R^2 \tag{5}$$

where R denotes the bending radius. Finally, the bending radius of the substrate profile is calculated by using Eq. (5).

3. CCD image feedback control

According to a series of image processing, the bending radius of substrates can be measured in real time by CCD image. This study measures bending characteristics of substrates under different

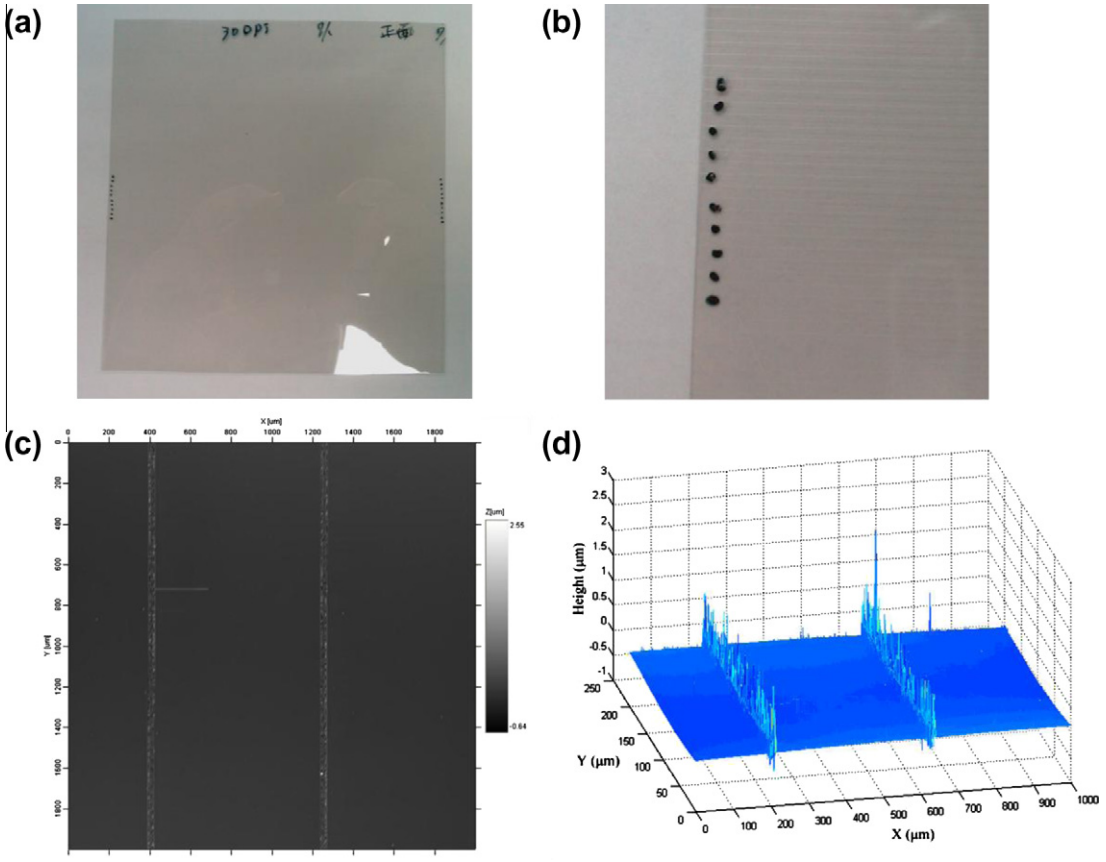

Fig. 10. (a) The entire picture, (b) zoom-in picture with electrodes, (c) stylus-instrument picture, and (d) 3-D height diagram of the PET/ITO sample measured by using a profilometer.

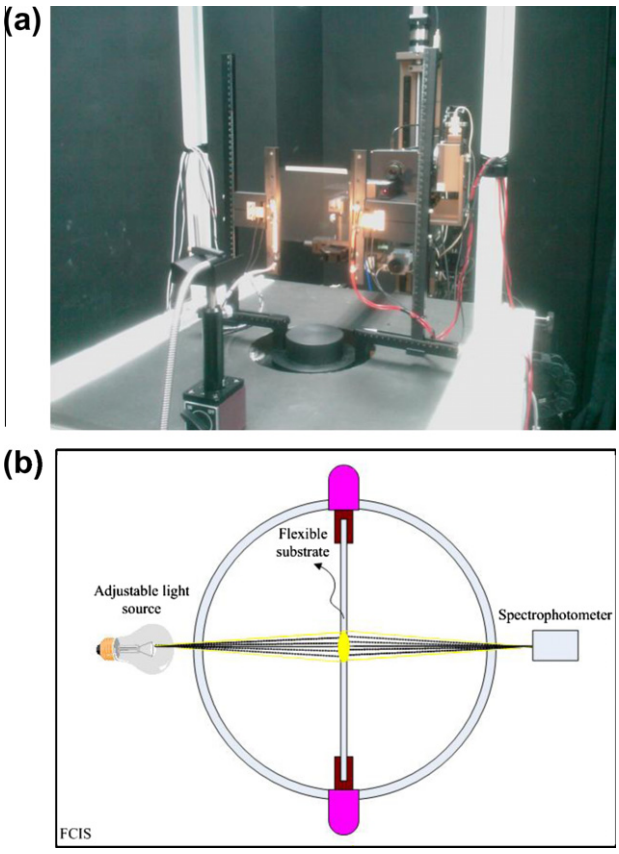

Fig. 11. (a) Photo and (b) schematic diagram of optical-transmittance characteristic measurement.

radii of curvature. Therefore, a control system is required to automatically adjust the bending radius. In this study, a motor drives FCIS to bend the substrate and control its bending radius based on CCD image feedback signals. Fig. 7 depicts a control block diagram. Firstly, a reference input represents a desired bending radius. Then, an input of the motor controller is equal to the value of subtracting the bending-radius feedback signal from the reference input. The input through a motor controller drives FCIS to bend the substrate. A CCD is used to measure the bending radius as the feedback signal. Finally, the bending-radius feedback control is complete when the bending-radius feedback signal is equal to the reference input within a tolerance. For example, Fig. 8 depicts bending radius and input voltage in experimental results of bending radius variation from 4 to 2 cm. The green line represents reference input, the blue line is the system output, and the magenta line is the drive voltage for FCIS. According to Fig. 8, this proposed image feedback control (IFC) facilitates controlling the bending radius of the substrate.

Because the bending radius control is one of major tasks in this study, 1 and 2 cm bending radius control are implemented for 75×75 mm and 125×125 mm PET substrates, respectively, by using IFC, as shown in Table 1. In Table 1, the maximum error of the bending radii is 0.05 cm, which is small enough in bending radius control.

Fig. 9 shows the procedure of measuring flexible samples. After the procedure, an aging data depicted in Table 2 is established for bending characteristics of substrates under different radii of curvature. Accordingly, aging data of bending characteristics depicted on flexible electronics help a designer or maker of flexible display design useful and comfortable flexible electronic products.

4. Experiment

Because the flexible display is bendable, a flexible back plate is used to drive the display media, e.g., Cholesteric Liquid Crystal (Ch-LC) and Organic Light Emitting Diode (OLED). Therefore, this study investigates characteristics of the substrate in bending. In order to measure electrical characteristics of the substrate under different radii of curvature, a commercially available ITO-coated PET (OCTM 100) from CPFilms Inc. is utilized. It has 50 nm think ITO on a 125-μm-think PET sheet. A laser writer is used in this work to make line patterns on a PET/ITO sample. Each line pattern is an ITO-line pattern separated by an isolation pattern. For example, Fig. 10 shows a

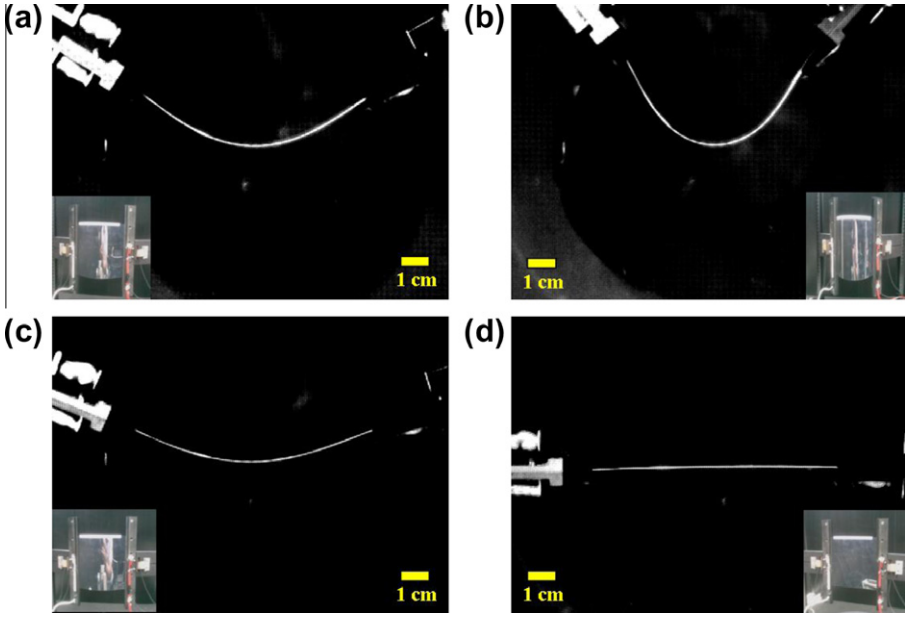

Fig. 12. Four photos of (a), (b), (c), and (d) in order within one bending cycle by using FCIS to obtain 2 cm bending radius.

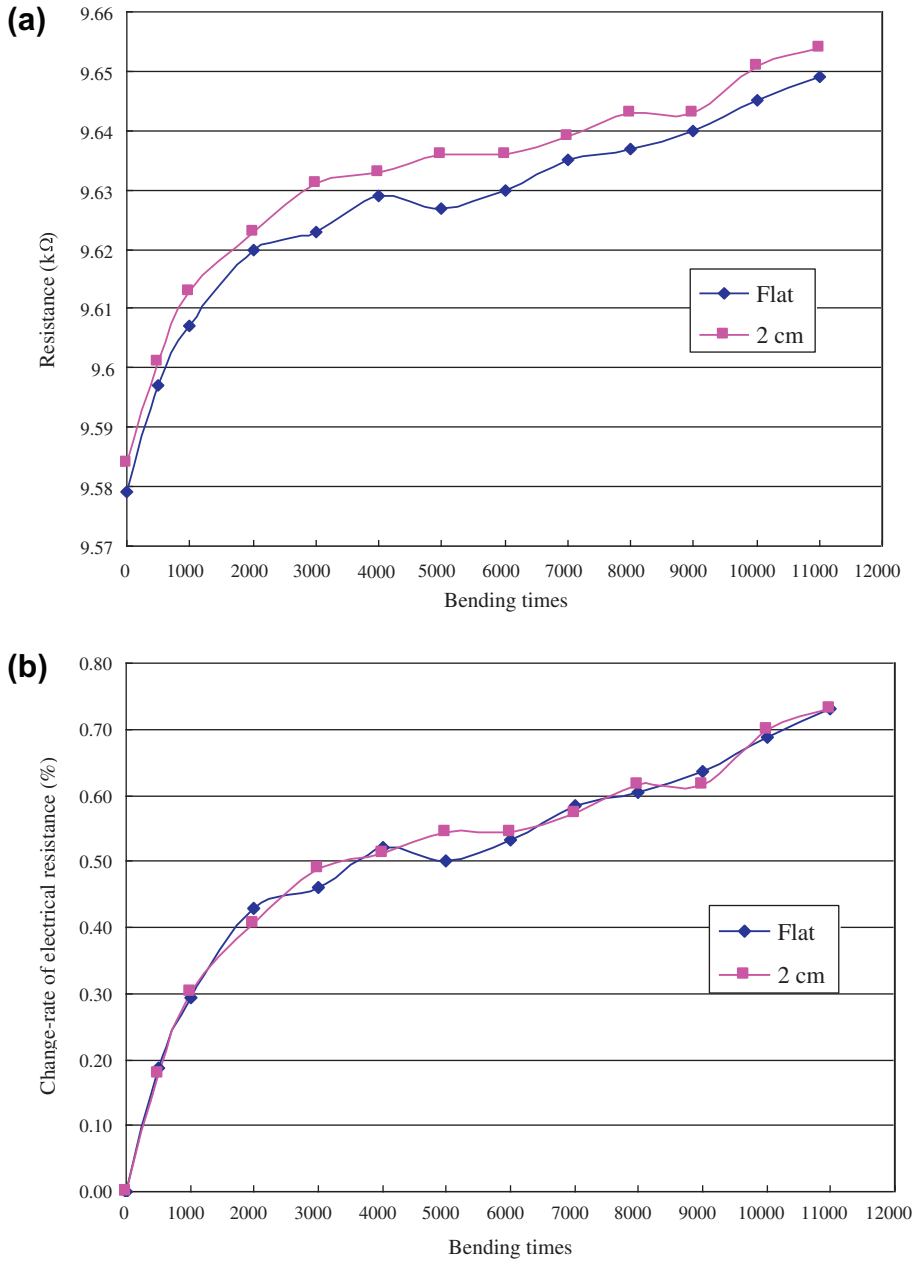

Fig. 13. (a) Electrical-resistance measurement and (b) change-rate of electrical resistance of 30 dpi flexible PET/ITO sample in flat and 2 cm bending radius conditions up to 11,000 bending times.

30 dpi-wide line pattern on the sample. The length and width of the sample are 125 mm and 125 mm, respectively. The distance between lines on the line pattern is 817 μm. The average roughness of the line pattern is around 30 nm. The highest height of the isolation pattern done by the laser writer is 1.5 μm according to Fig. 10d. Therefore, in FCIS the method of 4-point-probe electrical-resistance measurement based on IFC is applied for measuring the electrical resistance of the line pattern.

On plastic substrates of flexible display, HMDSO films can be employed as protective anti-scratch coatings. Therefore, a 125 μm thick PET sheet with 200 nm thick HMDSO plasma-polymerized thin films is utilized for optical-characteristic measurement, as shown in Fig. 11, in which light source A and a spectrometer are utilized. The area of optical-transmittance characteristic measurement is 2 cm radius circle at the middle of the sample. By using FCIS based on IFC, this study successfully carried out optical-transmittance characteristic measurement of flexible PET/HMDSO substrates up to 5000 bending times with the same radius of curvature.

5. Results and discussion

Fig. 12 shows in a bending cycle four sequential photos obtained by using IFC to control 2 cm bending radius. Therefore, a 30 dpi flexible PET/ITO sample was measured in flat and 2 cm bending radius conditions, respectively, for bending 11,000 times by using FCIS, as shown in Fig. 13. Table 2 shows aging results in electrical-resistance measurement of 30 dpi flexible PET/ITO sample in flat and 2 cm bending radius conditions up to 11,000 bending times. The maximum error of the bending radii is 0.05 cm in

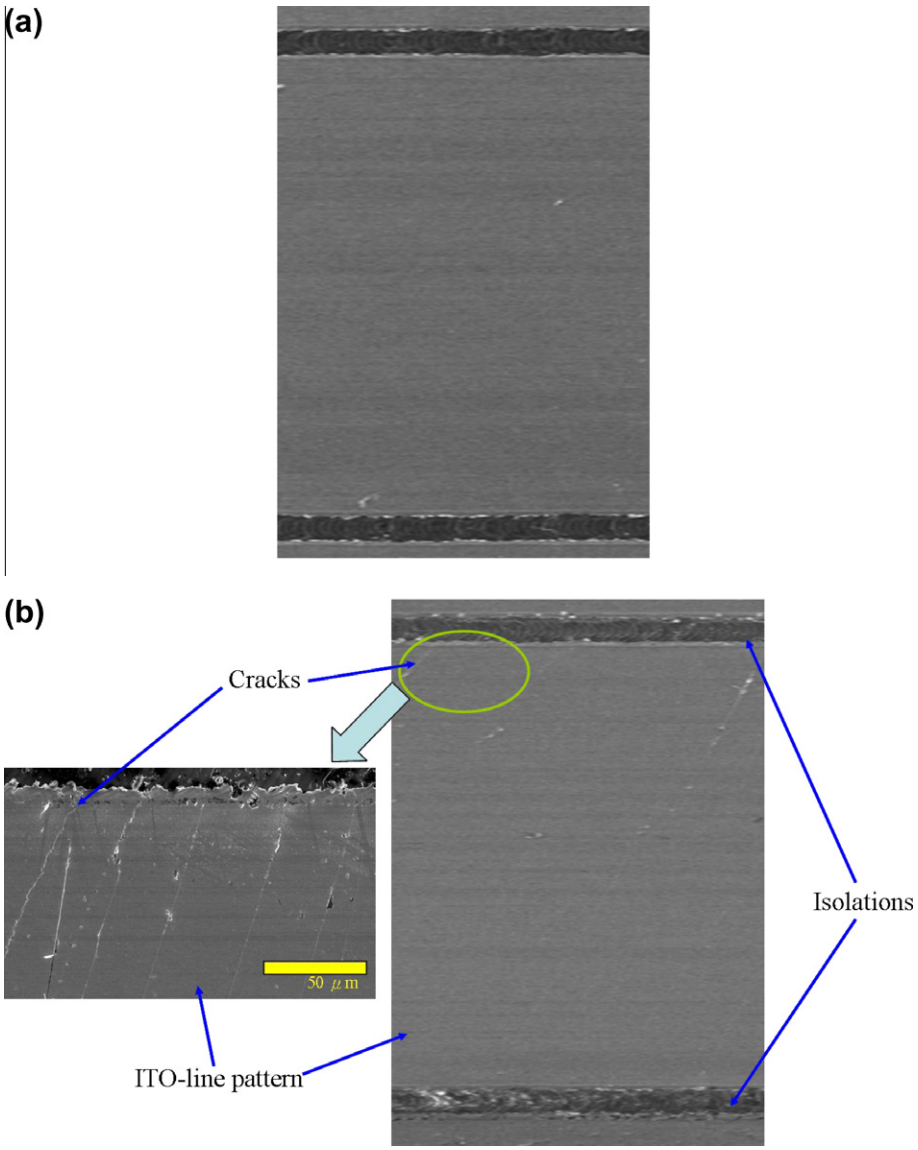

Fig. 14. (a) SEM photo before bending and (b) cracks on the line pattern of PET/ITO sample after 11,000 bending times.

bending radius control. Fig. 13a depicts that the sample resistance with 2 cm bending radius is larger than flat one [1], because the ITO-line pattern becomes thinner in bending. In addition, Fig. 13b depicts that as the bending times increase, the change-rate of electrical resistance in both flat and 2 cm bending radius conditions also increase, where change-rates are calculated from the difference of the electrical resistance of the line pattern between before and after bending divided by the electrical resistance before bending.

Because the bending direction is perpendicular to the ITO-line-pattern direction, tension stress [20] in the PET/ITO sample generates line cracks on the ITO-line pattern, as shown in Fig. 14, or makes the ITO-line pattern thinner. When there are cracks on the ITO-line pattern or the ITO-line pattern becomes thinner, the cross-sectional area that allows electric current passes on the ITO-line pattern becomes smaller. According to Ohm's law [21], the electrical resistance of the ITO-line pattern increases. Hence, electrical resistance of the ITO-line pattern increases due to repetitive bending.

In addition, this study has successfully measured optical-transmittance characteristics of PET/HMDSO substrates up to 5000 bending times with 2 cm radius of curvature, as shown in Fig. 15. As a result, as the bending times increase, the optical transmittance becomes higher, since there appear some cracks on the top film after thousands of bending times [22]. Accordingly, the cracks make the HMDSO film thinner on the cracks. It is easier to leak the light through the PET/HMDSO substrate. Therefore, the optical transmittance of the PET/HMDSO substrate becomes higher after 5000 bending times than one without bending operation.

6. Conclusions

This study has quantized the bending condition of substrates by using IFC. This study also has measured the electrical and optical properties of substrates by using FCIS. Measurement results are crucial to development of flexible display technology. Accordingly, FCIS is a good tool for inspection of flexible displays under bending situations to help a designer or maker of flexible displays design useful and comfortable flexible electronic products.

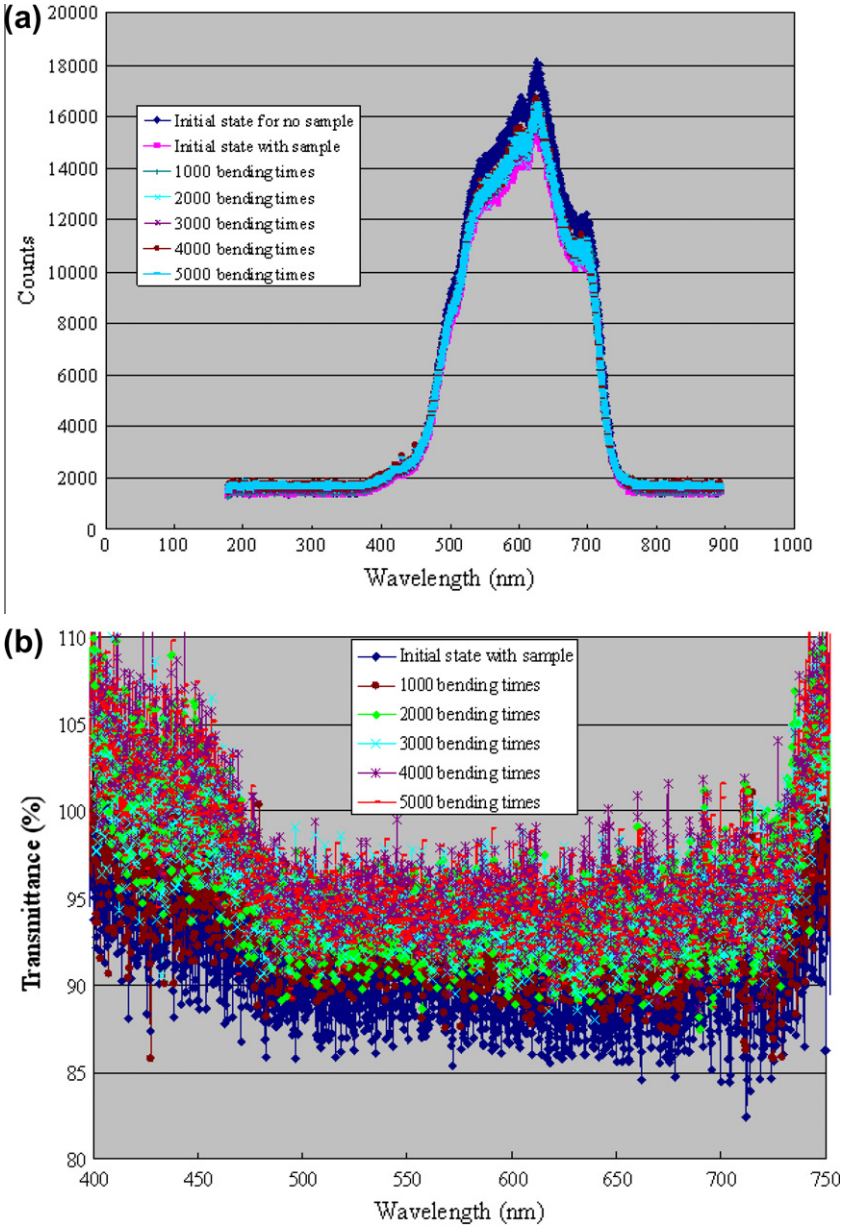

Fig. 15. (a) Spectrum results and (b) optical-transmittance results for optical measurement of flexible PET/HMDSO substrates up to 5000 bending times under 2 cm radius of curvature.

Acknowledgment

Thanks for Display Technology Center of Industrial Technology Research Institute who provides flexible substrates.

References

[1] S. Grego, J. Lewis, E. Vick, D. Temple, Development and evaluation of bend-testing techniques for flexible-display applications, J. SID 13 (2005) 575–581.
[2] J.S. Lewis, S. Grego, E. Vick, et al., Highly flexible transparent electrodes for organic light-emitting device (OLED) based displays, Appl. Phys. Lett. 85 (2004) 34–50.
[3] J.S. Lewis, S. Grego, E. Vick, et al., Mechanical performance of thin films in flexible displays, Mater. Res. Soc. Symp. Proc. 814 (2004) 14–18.
[4] M.J. Matthewson, C.R. Kurkjian, S.T. Gulati, Strength measurement of optical fibers by bending, J. Am. Ceram. Soc. 69 (1986) 8–15.
[5] Q. Chen, L. Xu, A. Salo, Reliability study of flexible display module by experiments, in: International Conference on Electronic Packaging Technology and High Density Packaging, 2008, pp. 1–6.
[6] S. Kurosawa, B.-G. Choi, J.-W. Park, H. Aizawa, K.-B. Shim, K. Yamamoto, Synthesis and characterization of plasma-polymerized hexamethyldisiloxane films, Thin Solid Films 506–507 (2006) 176–179.
[7] L. Zajickova, V. Bursikova, Z. Kucerova, J. Franclova, P. Stahel, V. Perina, A. Mackova, Organosilicon thin films deposited by plasma enhanced CVD: thermal changes of chemical structure and mechanical properties, J. Phys. Chem. Solids 68 (2007) 1255–1259.
[8] R. Morenta, N. De Geytera, S. Van Vlierbergheb, P. Dubruelb, C. Leysa, L. Gengembrec, E. Schachtb, E. Payenc, Deposition of HMDSO-based coatings on PET substrates using an atmospheric pressure dielectric barrier discharge, Prog. Org. Coat. 64 (2009) 304–310.
[9] A.A. Meier, D.I. Levinzon, Application of the four-probe method for measuring the resistivity of nonuniform semiconductor materials, Meas. Tech. 8 (5) (1965) 427–429.
[10] Q.Z. Wu, B.S. Jeng, Background subtraction based on logarithmic intensities, Pattern Recogn. Lett. 23 (2002) 1529–1536.
[11] K. Kima, T.-H. Chalidabhongseb, D. Harwooda, L. Davis, Real-time foreground-background segmentation using codebook model, Real-Time Imag. 11 (2005) 172–185.
[12] Z. Zivkovic, F. Heijden, Efficient adaptive density estimation per image pixel for the task of background subtraction, Pattern Recogn. Lett. 27 (2006) 773–780.
[13] Y.D. Qu, C.S. Cui, S.B. Chen, J.Q. Li, A fast subpixel edge detection method using Sobel–Zernike moments operator, Image Vis. Comput. 23 (2005) 11–17.

[14] C.C. Kanga, W.J. Wanga, Anovel edge detection method based on the maximizing objective function, Pattern Recogn. 40 (2007) 609–618.
[15] X. Xu, Z. Yang, Y. Wang, A method based on rank-ordered filter to detect edges in cellular image, Pattern Recogn. Lett. 30 (2009) 634–640.
[16] I. Sobel, Neighbourhood coding of binary images fast contour following and general array binary processing, Comput. Vision Graph. 8 (1978) 127–135.
[17] N. Otsu, A threshold selection method from gray level histograms, IEEE Trans. Syst. Man, Cybern. 9 (1) (1979) 62–66.
[18] R.C. Gonzalez, R.E. Woods, Digital Image Processing, Prentice Hall, 2002.
[19] L. Shapiro, G. Stockman, Computer Vision, Prentice Hall, 2002.
[20] J.M. Gere, S.P. Timoshenko, Mechanics of Materials, International Thomson Publishing, 1997.
[21] L.S. Lerner, Physics for Scientists and Engineers, Jones & Bartlett, 1997.
[22] Y.L. Chen, H.C. Hsieh, W.T. Wua, B.J. Wen, W.Y. Chang, D.C. Su, An alternative bend-testing technique for a flexible indium tin oxide film, Displays 31 (2010) 191–195.